

Exponential growth of out-of-time-order correlator of regular orbits

Shangyun Wang^{1*}, Songbai Chen^{2,3†}, Jiliang Jing^{2,3 ‡}

¹*College of Physics and Electronic Engineering,*

Hengyang Normal University, Hengyang 421002, China

²*Department of Physics, Key Laboratory of Low Dimensional
Quantum Structures and Quantum Control of Ministry of Education,
Synergetic Innovation Center for Quantum Effects and Applications,*

Hunan Normal University, Changsha, Hunan 410081, People's Republic of China

³*Center for Gravitation and Cosmology, College of Physical Science and Technology,
Yangzhou University, Yangzhou 225009, People's Republic of China*

Abstract

We have studied the early behavior of out-of-time-order correlator (OTOC) in two non-chaotic inverted harmonic oscillator systems. It is shown that there exist behaviors of exponential growth of OTOC. The classical-quantum correspondence in the inverted harmonic oscillator (IHO) system depends not only on the photon number of system, but also on the central position of the initial state in phase space. Moreover, we analyze the Husimi quasi-probability wave packets of different initial states during the OTOC grows exponentially in both inverted harmonic oscillator systems, and find that the center of corresponding quantum wave packets spreads along the classical phase trajectory. Particularly, we find that the wave packets related to the classical particle moving along stable regular orbits diffuse rapidly so their OTOCs grow exponentially before the Ehrenfest time. Our results could help to further understand the classical-quantum correspondence and OTOC.

PACS numbers: 42.50.Pq, 05.45.Mt, 73.43.Nq

* Corresponding author: sywang@hynu.edu.cn

† csb3752@hunnu.edu.cn

‡ jljing@hunnu.edu.cn

I. INTRODUCTION

The exponential growth of out-of-time-order correlator (OTOC) has been regarded as a indicator of chaos or quantum instability in many quantum systems[1–15]. In particular, its growth rate is closely associated with the classical Lyapunov exponent(CLE) λ in the large N limit[12–18]. In the context of black holes physics, the OTOC can be considered to as an indicator of chaos in gravity dual theory [19] and the corresponding upper bound of the maximum quantum Lyapunov exponent (QLE) is obtained in black hole geometry [1, 20, 21]. Experimentally, the OTOC has been measured in the ion traps systems[22–25] and in the nuclear magnetic resonance platforms[26–28].

However, an important discovery is that the OTOC in some non-chaotic regular systems also shows exponential growth behavior in early time and the fast scrambling emerges not only in the chaotic case but also in the regular one[29]. In the integrable systems, it is shown that the OTOC at the saddle points (unstable fixed points) could grow exponentially [30] due to the quantum instability existing in the vicinity of these points [31]. The similar behavior of OTOC also appears in the inverted harmonic oscillator system with a Higgs potential[32]. It is not surprising because the instability of the unstable fixed point causes its CLE to be positive. Then, it is natural to ask whether unstable regular orbits lead the OTOC shows exponential growth behavior in early time. To study the early behavior of OTOC of unstable regular orbits, we consider the simplest unstable but regular system — the inverted harmonic oscillator system, described by the Hamiltonian $\hat{H} = p^2/2m - m\omega^2 q^2/2$ [33]. This special system has been widely studied in various aspects. It is shown that this regular system has an exponential sensitivity to initial conditions as in the chaotic systems[34]. The phase-space volume of the classical inverted harmonic oscillator is unbounded, however, its corresponding volume for quantum inverted oscillator can be bounded by the system photons[35, 36]. Especially, the inverted harmonic oscillator is not just a pure theoretical model and has been realized experimentally[37]. In mathematics, it even challenges the Riemann hypothesis[38]. Moreover, it also shows important significance in both general relativity, quantum mechanics and chaotic domain[39–45].

Fidelity OTOC (FOTOC) is related to the quantum variance of a Hermitian operator on the initial state and is also shown to be associated with the CLE of chaotic systems[13] and the quantum instability of saddle point in non-chaotic system [31]. The FOTOC provides a method for us to visualize the chaotic or scrambling dynamics of a quantum system in semi-classical phase space. In Schrodinger picture, the evolution of the quantum wave packet in the phase space will be directly related to the quantum variance of momentum

or coordinate operator. On the other hand, Husimi Q function is one of the quasi-probability distribution functions and was used to visualize the evolution of quantum wave packets in phase space[46–50]. In this paper, we will study the early evolution of Husimi quasi-probability wave packets in two inverted harmonic oscillator systems and to see what Husimi quasi-probability wave packets behave as the OTOCs grow at an exponential rate.

This paper is organized as follows. In section II, we study the relationship between the mean photon number and the bounded region in quantum IHO system. In section III, we analyze the early behavior of OTOC of unstable regular orbits in IHO system and visualize the OTOC by Husimi Q function. In section IV, we study the false chaotic signal of stable regular orbit and explain it by Husimi Q function. Finally, we present results and a brief summary.

II. MEAN PHOTON NUMBER IN INVERTED HARMONIC OSCILLATOR

In this section, we study the classical one-dimensional IHO system with unstable regular orbits, namely,

$$H = \frac{p^2}{2m} + \hat{V}, \quad V = -\frac{1}{2}m\omega^2 q^2, \quad (1)$$

where ω and m are the frequency and mass of IHO, respectively. In contrast to harmonic oscillator, the

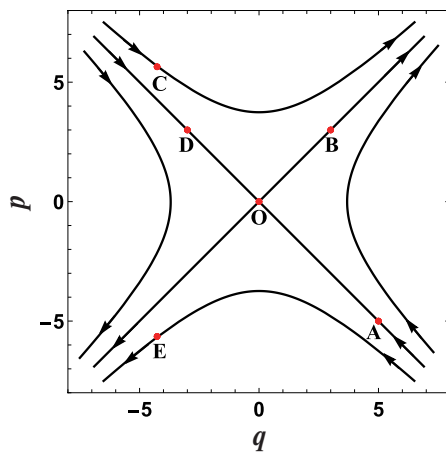


FIG. 1: The classical dynamics phase diagram of IHO. The coordinate (q, p) of points O, A, B, C, D and E are $(0, 0), (5, -5), (3, 3), (-4.267, 5.643), (-3, 3)$ and $(-4.267, -5.643)$, respectively. Point O is the saddle point.

potential V tends to infinity in the limit $q \rightarrow \infty$. In Fig. 1, we present the classical dynamics phase diagram of IHO system. For the classical system (1), there is a saddle point ($q = 0, p = 0$) in phase space. The particle starting from initial point on the asymptote ($p = -q$) moves to the saddle point and the corresponding orbit is stable, which forms a so-called stable manifold. The particle starting from other points moves to infinity

and its orbit is unstable, but its CLE is the same as that from the saddle point, i.e. $\lambda_O = 1$.

To study the quantum dynamics of IHO, we introduce the quadratic quantization form of the position and momentum operators and set $\hbar = m = \omega = 1$,

$$x = (a^\dagger + a)/\sqrt{2}, \quad p = i(a^\dagger - a)/\sqrt{2}, \quad (2)$$

and then the quantum Hamiltonian of IHO becomes

$$\hat{H} = -\frac{1}{2}(a^2 + a^{\dagger 2}). \quad (3)$$

Notice that the Hamiltonian (3) is equivalent to the Hamiltonian (1) in the classical limit where the system photon number $N_p \rightarrow \infty$. As in Refs.[47, 51], we take the photon coherent state as the initial state of system

$$|\psi\rangle = e^{-\beta\beta^*/2} e^{\beta a^\dagger} |0\rangle, \quad (4)$$

with

$$\beta = (q + ip)/\sqrt{2}. \quad (5)$$

where $|0\rangle$ is the ground state of light field, q and p are generalized coordinates and momentum. According to quantum theory, the mean photon number on the initial coherent state is

$$\langle a^\dagger a \rangle = \langle \psi | a^\dagger a | \psi \rangle = \beta\beta^\dagger = (q^2 + p^2)/2. \quad (6)$$

Eq.(6) implies that the mean photon number is related to the center position of coherent state in phase space. In other words, if the photon number of the system N_p is given, the coordinate and momentum parameters of coherent states in phase space are bounded in the region $(q^2 + p^2)/2 \leq N_p$. This shows that there is a natural boundary in phase space of the quantum IHO system with finite photon number, while the corresponding classical IHO system is unbounded because in the classical limit $N_p \rightarrow \infty$.

Taking a coherent state centering at the point B in Fig. 1 as the initial value, we present the mean photon number evolution with time for different initial photon number N_p , as shown in Fig. 2(a). We find that the mean photon number $\langle a^\dagger a \rangle$ keeps increasing with the time in the classical limit case $N_p \rightarrow \infty$. For the case with finite initial photon number N_p , the curve of mean photon number changing with time (i.e., $\langle a^\dagger a \rangle - t$) first overlaps that in the classical limit. After a time t_p , the mean photon number decreases and does not change with time along the line in the classical limit. This means that during the period $0 < t \leq t_p$ there exists the so-called classical-quantum correspondence for the system (1) because as $t > t_p$ the quantum behavior in

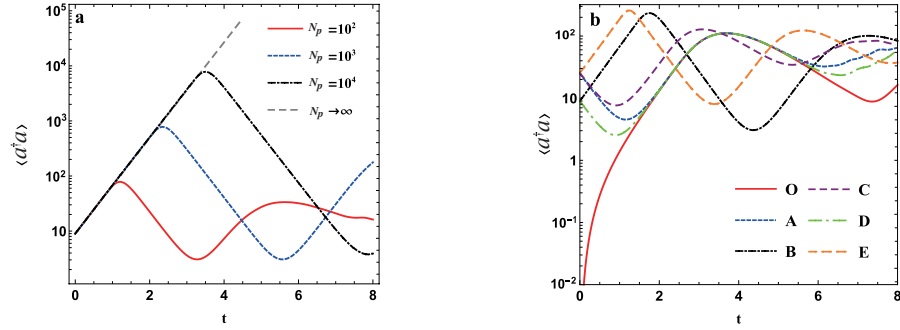


FIG. 2: Time evolution of the mean photon number. (a) Plots of the mean photon number for point B in Fig. 1 with different system photon number. (b) Plots of the mean photon number for six different points [as marked in Fig. 1] with fixed system photon number $N_p = 300$.

the system differs from that in the classical system. We also note that the time t_p increases with the initial photon number N_p , which is understandable because the classical-quantum correspondence becomes clearer in the system with larger photon number. Moreover, the largest mean photon number N_{lm} maintaining the classical-quantum correspondence is less than the initial photon number N_p . Strictly, this also implies that the maintaining of classical-quantum correspondence is determined by the largest mean photon number N_{lm} rather than the initial photon number N_p .

In Fig. 2(b), we exhibit the mean photon number $\langle a^\dagger a \rangle$ evolution with time for different initial points in Fig. 1. It is shown that the change of mean photon number depends on the center position of the quantum wave packets in phase space. For the starting points located in the stable manifold of the saddle point, such as point A, C, and D, the mean photon number $\langle a^\dagger a \rangle$ decreases firstly and then increases to the maximum value. For the starting points located in the unstable manifold, the mean photon number directly grows to the maximum. Moreover, Fig. 2 also implies that the length of time maintaining classical-quantum correspondence in the quantum IHO depends else on the center positions of the initial coherent states of system in the phase space.

III. EXPONENTIAL GROWTH OF OTOC IN INVERTED HARMONIC OSCILLATOR

In this section, we study the quantum variance derived from the OTOC in the IHO system and analyse the Husimi quasi-probability wave packet during the OTOC growth exponentially. The OTOC is defined as[53]

$$C(t) = \langle [\hat{W}(t), \hat{V}(0)]^\dagger [\hat{W}(t), \hat{V}(0)] \rangle, \quad (7)$$

where $\langle \dots \rangle$ denotes the expectation values and $\hat{W}(t) = e^{i\hat{H}t} \hat{W} e^{-i\hat{H}t}$. \hat{H} is a quantum Hamiltonian, \hat{W} and \hat{V} are two arbitrary local operators. Here, we choose $\hat{W} = \hat{P} = i(a^\dagger - a)/\sqrt{2}$ and \hat{V} as a projection operator onto the initial state $|\psi\rangle$, i.e., $\hat{V} = |\psi\rangle\langle\psi|$. Substituting the operators $\hat{V} = |\psi\rangle\langle\psi|$ and $\hat{W} = \hat{P}$ into the Eq.

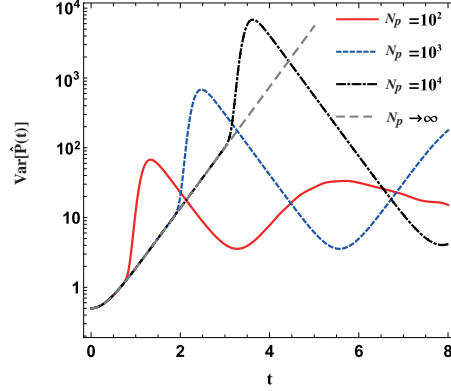


FIG. 3: Time evolution of the OTOC for point B in Fig. 1 with different system photon number.

(7), one has

$$C(t) = \langle \psi(t) | \hat{P}^2 | \psi(t) \rangle - \langle \psi(t) | \hat{P} | \psi(t) \rangle^2 \equiv Var[\hat{P}(t)], \quad (8)$$

where $Var[\hat{P}(t)]$ is the quantum variance of the momentum operator \hat{P} . This relation is similar to the

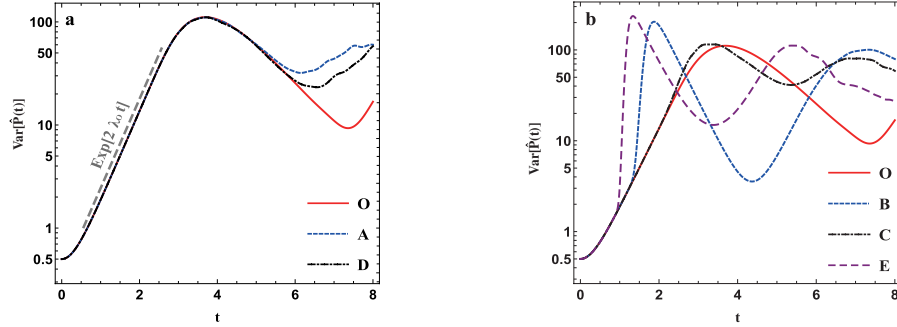


FIG. 4: Time evolution of the OTOC for the initial coherent states centered at different points. The gray dashed line in the left panel corresponds to the exponential growth rate given by twice the classical Lyapunov exponent. Here, we set the system photon number $N_p = 300$.

definition of FOTOC[13] and enable us to visualize the OTOC in semiclassical phase space. In Fig. 3, we find that the exponential growth rate $\tilde{\lambda}$ of OTOC is independent of system photon number N_p , and the time to keep $Var[\hat{P}(t)]$ growing exponentially increases with N_p . For the initial state centered at the point in the stable manifold, the evolution of OTOC with time is completely consistent before the Ehrenfest time $\tau = \frac{1}{\tilde{\lambda}} \ln N_p$, and the exponential growth rate is twice the CLE of saddle point, i.e. $\tilde{\lambda} = 2\lambda_O$, as shown in Fig. 4(a). For the initial state centered at the point in the unstable manifold, in Fig. 4(b), we find that the time of the OTOC owning the same exponential growth rate as the saddle point depends on the position of the initial state in the phase space. From the view of the evolution of the OTOC, Figs. 3 and 4(b) further illustrate that both the photon number of system and the position of the initial coherent state affect the classical-quantum

correspondence in the IHO system.

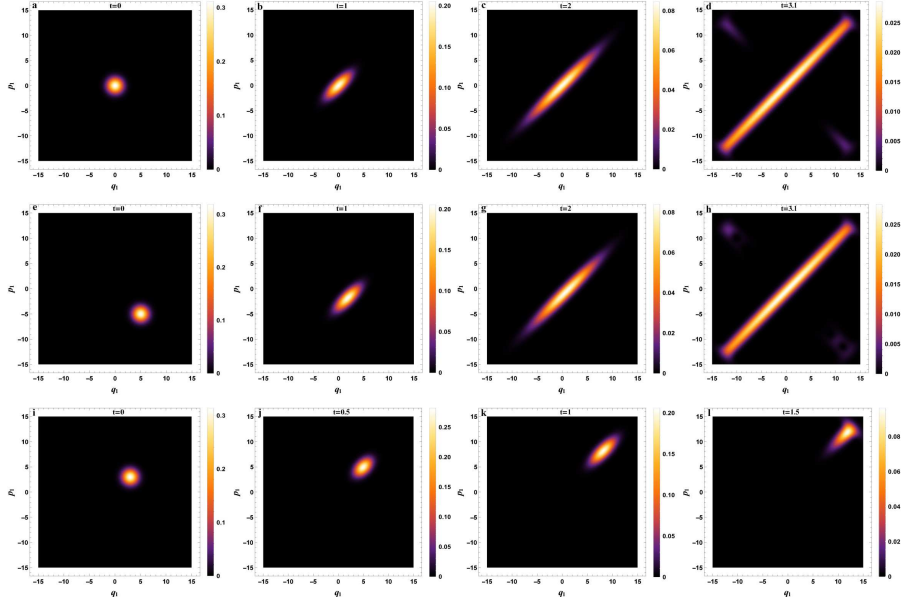


FIG. 5: Change of Husimi quasi-probabilistic wave packets with time for fixed system photon number $N_p = 300$. The top, middle and bottom panels denote respectively the case in which the initial coherent state centered at the points O , A and B in Fig. 1.

Husimi Q function is one of the quasi-probability distribution functions, and it was used to distinguish chaotic and periodic orbits in quantum systems[46–51]. The definition of Husimi Q function is

$$Q(q_1, p_1) = \frac{1}{\pi} \langle q_1, p_1 | \rho | q_1, p_1 \rangle, \quad (9)$$

where $|q_1, p_1\rangle$ is photon coherent state and ρ is the density matrix. In Fig. 5, we present the change of Husimi Q distribution in phase space for the IHO system with different initial values. Figs. 5(a)-5(c) and 5(e)-5(g) show that the change of quasi-probability wave packets for the initial points in the stable manifold own similar behaviors during the OTOC grows exponentially. This means that the evolution of OTOC associated with the initial states centre on stable manifold are highly consistent before the Ehrenfest time, which is also shown in Fig. 4(a). In Figs. 5(i)-5(l), we show that the evolution of Husimi quasi-probabilistic wave packet with the initial state centered at point B located on the unstable manifold. It is found that the time reduces for the wave packet owning the behaviors similar to that on stable manifold. Actually, during the OTOC grows exponentially, it is easy to find that in the IHO system, the corresponding quantum wave packets spread along the phase trajectory in the classical phase space. In addition, we present the Husimi quasi-probabilistic wave packets after the OTOC grows exponentially in Figs. 5(d), 5(h) and 5(l) for points O , A and B . We find that some discrete wave packets appear outside the primary wave packet and there is no the corresponding

classical states, which is different from those during the OTOC exhibits exponential growth behavior.

IV. EXPONENTIAL GROWTH OF OTOC IN INVERTED HARMONIC OSCILLATOR WITH HIGGS POTENTIAL

In this section, we focus on the inverted harmonic oscillator with a Higgs potential[32], which is classically non-chaotic but a nonzero CLE appears at the the unstable maximum of the potential. We find that the OTOC of stable regular orbit far from the saddle point also grows exponentially in early time. The one-dimensional

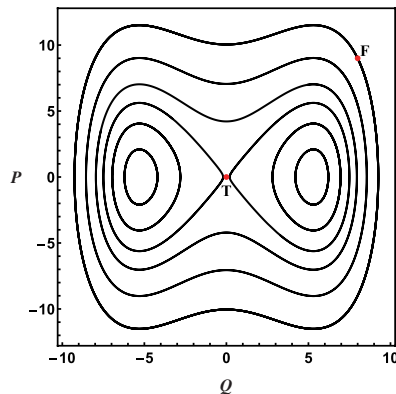


FIG. 6: The classical dynamics phase diagram of HIHO. Point T is the saddle point and point F (8, 9) is a point on a periodic orbit far away from the saddle point. Here, we set $\gamma = 3$ and $g = 1/25$.

inverted harmonic oscillator including the Higgs potential (HIHO) is described by the Hamiltonian

$$H \equiv P^2 + \hat{V}, \quad V \equiv -\frac{1}{4}\gamma^2 Q^2 + gQ^4 + \frac{\gamma^4}{64g}, \quad (10)$$

where γ and g are constant parameters and the term Q^4 ensures the existence of the potential boundary. There is a saddle point T . According to Jacobian matrix theory[52] and the tangent-space method[54], we calculate the CLE for the saddle point T and the other point F far from the point T , and find that $\lambda_T = \gamma$ and $\lambda_F = 0$, respectively. Substituting the quadratic quantization form of position and momentum operators into Hamiltonian (10), one can obtain the quantum Hamiltonian of HIHO

$$\hat{H}' = -\frac{1}{2}(a^\dagger - a)^2 - \frac{1}{8}\gamma^2(a^\dagger + a)^2 + \frac{g}{4}(a^\dagger + a)^4 + \frac{\gamma^4}{64g}. \quad (11)$$

In Fig. 7, we find that the mean photon number in HIHO first oscillates and then tends to the saturate. Moreover, the evolution of the mean photon number with time is indistinguishable when the system photon number is larger than 250. Thus, in the HIHO system with $\gamma = 3$ and $g = 1/25$, the system photon number

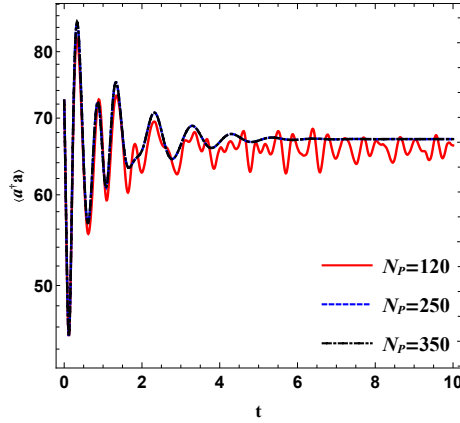


FIG. 7: Time evolution of the mean photon number for the initial state centering at the point F in Fig. 6 with different system photon number. Here, we set $\gamma = 3$ and $g = 1/25$.

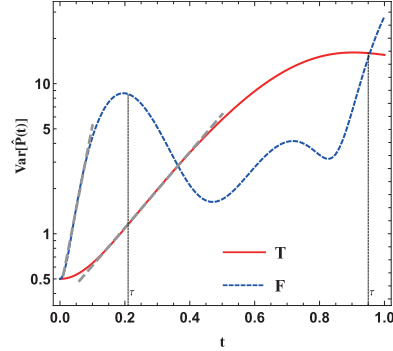


FIG. 8: Time evolution of the OTOC for the initial state entered at the saddle point T and the point F in Fig. 6. The gray dotted line is the fitting curve. Here, we set $N_p = 250$, $\gamma = 3$ and $g = 1/25$.

$N_p = 250$ can satisfy the requirement of photon number of quantum dynamics evolution. Similarly, the OTOC at saddle point shows exponential behavior at early time due to the inherently instability as in IHO. However, for the regular point F , the evolution of the OTOC also grows exponentially and its growth rate $\tilde{\lambda}_F \approx 25.52$, which is larger than that of the saddle point, as shown in Fig. 8. In particular, the exponential growth behavior of OTOC for the initial state entered at point F also occurs before the corresponding Ehrenfest time $\tau = \ln(N_p)/\tilde{\lambda}_F \approx 0.22$, which exacerbates the difficulty of discriminating chaos through OTOC.

We also study the early evolution behavior of the corresponding Husimi quasi-probabilistic wave packet in phase space. In Fig. 9, we find that during the OTOC grows exponentially, the quantum wave packets initially entered at points T and F spread along the phase trajectory in the classical phase space. Particularly, for the stable point F , the Husimi quasi-probabilistic wave packet diffuse rapidly along the vertical axis in phase space as the OTOC grows at an exponential rate, as shows in Figs. 9(e)-9(h). This rapid change of wave packet in a short time leads the quantum variance of momentum operator increases sharply, which lead

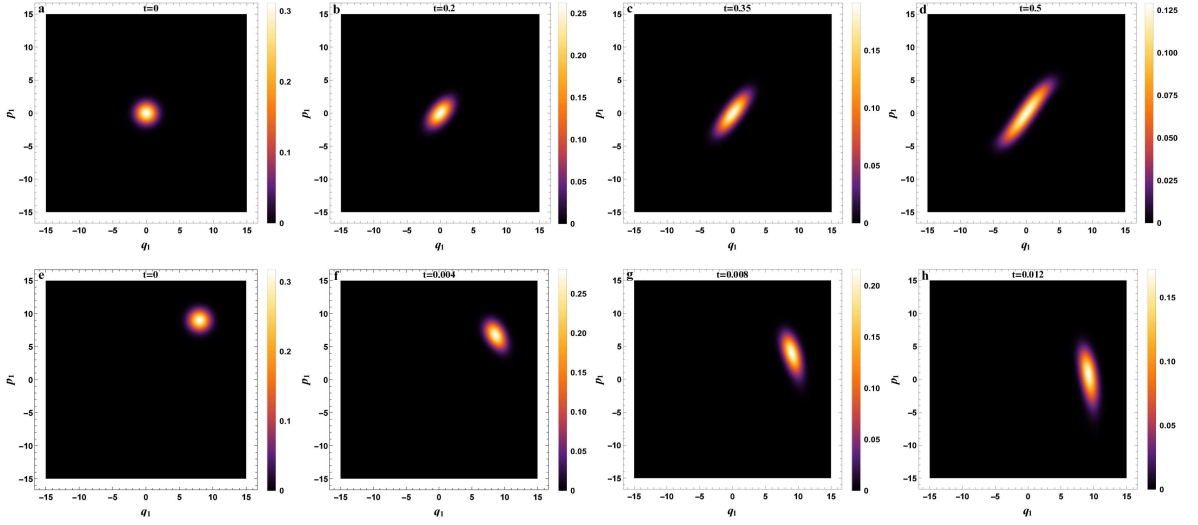


FIG. 9: Change of Husimi Q distribution with time for fixed system photon number $N_p = 250$. Parts (a)-(d) denote the case in which the initial coherent state center at the saddle point T in Fig. 6. Parts (e)-(h) denote the case in which the initial coherent state center at stable point F in Fig. 6. Here, we set $\gamma = 3$ and $g = 1/25$.

the OTOC grows exponentially.

V. CONCLUSION

We have studied the early behavior of OTOC in two inverted harmonic oscillator system IHO and HIHO. It is shown the OTOC starting from the coherent states centred on the regular orbits possess the behaviors of exponential growth in these two systems. For the IHO system, the OTOC from of the coherent states centred on stable manifold has the same growth rates as that at the saddle point at the early time, and their exponential growth rates is twice the CLE of the saddle point. For the coherent states centred on the unstable manifolds of IHO, the behavior of OTOC deviating from exponential growth form appears more earlier than that in the stable manifold. Moreover, we find that both the system photon number and the position of the initial coherent state affect the classical-quantum correspondence relationship in IHO system. We analyze the Husimi quasi-probability wave packets of different initial states during the OTOC grows exponentially, and find that in both inverted harmonic oscillator systems, the corresponding quantum wave packets spread along the phase trajectory in the classical phase space. Particularly, in HIHO system, the quantum wave packets of stable regular orbits diffuse rapidly along the vertical axis in phase space, which leads the OTOC shows false chaotic signals. Our results could help to further understand the OTOC and correspondence principle.

VI. ACKNOWLEDGMENTS

-
- [1] S. H. Shenker and D. Stanford, Black holes and the butterfly effect, *J. High Energy Phys.* 03 (2014) 067.
- [2] D. A. Roberts and D. Stanford, Diagnosing Chaos Using Four-Point Functions in Two-Dimensional Conformal Field Theory, *Phys. Rev. Lett.* 115, 131603 (2015).
- [3] E. R. Castro et al, Quantum-classical correspondence of a system of interacting bosons in a triple-well potential, *Quantum* 5, 563 (2021).
- [4] M. Rautenberg and M. Gärttner, Classical and quantum chaos in a three-mode bosonic system, *Phys. Rev. A* 101, 053604 (2020).
- [5] Ben Craps et al, Lyapunov growth in quantum spin chains, *Phys. Rev. B* 101, 174313 (2020).
- [6] R. K. Shukla, A. Lakshminarayan, and S. K. Mishra, Out-of-time-order correlators of nonlocal block-spin and random observables in integrable and nonintegrable spin chains, *Phys. Rev. B* 105, 224307 (2022).
- [7] M. McGinley, A. Nunnenkamp, and J. Knolle, Slow Growth of Out-of-Time-Order Correlators and Entanglement Entropy in Integrable Disordered Systems, *Phys. Rev. Lett.* 122, 020603 (2019).
- [8] T. Akutagawa, K. Hashimoto, T. Sasaki, and Ryota Watanabe, Out-of-time-order correlator in coupled harmonic oscillators, *J. High Energy Phys.* 08 (2020) 013.
- [9] E. M. Fortes et al, Gauging classical and quantum integrability through out-of-time-ordered correlators, *Phys. Rev. E* 100, 042201 (2019).
- [10] R. K. Shukla, A. Lakshminarayan, and S. K. Mishra, Out-of-time-order correlators of nonlocal block-spin and random observables in integrable and nonintegrable spin chains, *Phys. Rev. B* 105 224307 (2022).
- [11] M. McGinley, A. Nunnenkamp, and J. Knolle, Slow Growth of Out-of-Time-Order Correlators and Entanglement Entropy in Integrable Disordered Systems, *Phys. Rev. Lett.* 122, 020603 (2019).
- [12] K. Hashimoto, K. Muratab, and R. Yoshii, Out-of-time-order correlators in quantum mechanics, *J. High Energy Phys.* 10 (2017) 138.
- [13] R. J. Lewis-Swan, A. Safavi-Naini, J. J. Bollinger, and A. M. Rey, Unifying scrambling, thermalization and entanglement through measurement of fidelity out-of-time-order correlators in the Dicke model, *Nat. Commun.* 10, 1581 (2019).
- [14] J. Chávez-Carlos et al, Quantum and Classical Lyapunov Exponents in Atom-Field Interaction Systems, *Phys. Rev. Lett.* 122, 024101 (2019).
- [15] A. V. Kirkova, D. Porrás, and P. A. Ivanov, Out-of-time-order correlator in the quantum Rabi model, *Phys. Rev. A* 105, 032444 (2022).
- [16] S. H. Shenker and D. Stanford, Black holes and the butterfly effect, *J. High Energy Phys.* 03 (2014) 067.
- [17] A. Bohrdt, C. B. Mendl, M. Endres, and M. Knap, Scrambling and thermalization in a diffusive quantum many-body system, *New J. Phys.* 19, 063001 (2017).
- [18] H. Shen, P. Zhang, R. Fan, and H. Zhai, Out-of-time-order correlation at a quantum phase transition, *Phys. Rev. B* 96, 054503 (2017).
- [19] J. M. Maldacena, The Large N limit of superconformal field theories and supergravity, *Int. J. Theor. Phys.* 38 (1999) 1113.
- [20] S.H. Shenker and D. Stanford, Multiple shocks, *J. High Energy Phys.* 12 (2014) 046.
- [21] J. Maldacena, S.H. Shenker, and D. Stanford, A bound on chaos, *J. High Energy Phys.* 08 (2016) 106.
- [22] M. Gärttner, J. G. Bohnet et al, Measuring out-of-time-order correlations and multiple quantum spectra in a trapped-ion quantum magnet, *Nat. Phys.* 13, 781 (2017).
- [23] K. A. Landsman, C. Figgitt et al, Verified quantum information scrambling, *Nature (London)* 567, 61 (2019).
- [24] M. K. Joshi, A. Elben et al, Quantum Information Scrambling in a Trapped-Ion Quantum Simulator with Tunable Range Interactions, *Phys. Rev. Lett.* 124, 240505 (2020).
- [25] A. M. Green, A. Elben et al, Experimental measurement of out-of-time-ordered correlators at finite temperature, *Phys. Rev. Lett.* 128, 140601 (2022).
- [26] J. Li, R. Fan, H. Wang, B. Ye, B. Zeng, H. Zhai, X. Peng, and J. Du, Measuring Out-of-Time-Order Correlators on a Nuclear Magnetic Resonance Quantum Simulator, *Phys. Rev. X* 7, 031011 (2017).
- [27] K. X. Wei, C. Ramanathan, and P. Cappellaro, Exploring Localization in Nuclear Spin Chains, *Phys. Rev. Lett.* 120, 070501 (2018).
- [28] M. Niknam, L. F. Santos, and D. G. Cory, Sensitivity of quantum information to environment perturbations measured with a nonlocal out-of-time-order correlation function, *Phys. Rev. Research* 2, 013200 (2020).
- [29] S. Pappalardi et al, Scrambling and entanglement spreading in long-range spin chains, *Phys. Rev. B* 98, 134303 (2018).
- [30] Saúl Pilatowsky-Cameo et al, Positive quantum Lyapunov exponents in experimental systems with a regular classical limit, *Phys. Rev. E* 101, 010202(R) (2020).
- [31] Tianrui Xu, Thomas Scaffidi, and Xiangyu Cao, Does Scrambling Equal Chaos?, *Phys. Rev. Lett.* 124, 140602 (2020).

- [32] K. Hashimoto, Kyoung-Bum Huh, Keun-Young Kimb, and Ryota Watanabea, Exponential growth of out-of-time-order correlator without chaos: inverted harmonic oscillator, *J. High Energy Phys.* 11 (2020) 068.
- [33] G. Barton, Quantum mechanics of the inverted oscillator, *Ann. Phys. (N.Y.)* 166, 322 (1986).
- [34] R. Blume-Kohout and W. Zurek, Decoherence from a chaotic environment: An upside-down oscillator as a model, *Phys. Rev. A* 68, 032104 (2003).
- [35] K. Gietka, T. Busch, Inverted harmonic oscillator dynamics of the nonequilibrium phase transition in the Dicke model, *Phys. Rev. E* 104, 034132 (2021).
- [36] K. Gietka, Squeezing by critical speeding up: Applications in quantum metrology, *Phys. Rev. A* 105, 042620 (2022).
- [37] S. Gentilini, M. C. Braidotti, G. Marcucci, E. DelRe, and C. Conti, Physical realization of the Glauber quantum oscillator, *Sci. Rep.* 5, 15816 (2015).
- [38] M. V. Berry and J. P. Keating, The Riemann zeros and eigenvalue asymptotics, *SIAM Rev.* 41, 236 (1999).
- [39] S. Choudhury et al, Four-mode squeezed states in de Sitter space: A study with two field interacting quantum system, arXiv:2203.15815.
- [40] Le-Chen Qu, Jing Chen, Yu-Xiao Liu, Chaos and Complexity for Inverted Harmonic Oscillators, *Phys. Rev. D* 105, 126015 (2022).
- [41] V. Subramanyan et al, Physics of the Inverted Harmonic Oscillator: From the lowest Landau level to event horizons, *Annals of Physics* 435 (2021) 168470.
- [42] Z. Tian et al, Verifying the upper bound on the speed of scrambling with the analogue Hawking radiation of trapped ions, *Eur. Phys. J. C* 82, 212 (2022).
- [43] Z. Lewis and T. Takeuchi, Position and Momentum Uncertainties of the Normal and Inverted Harmonic Oscillators under the Minimal Length Uncertainty Relation, *Phys. Rev. D* 84, 105029 (2011).
- [44] P. Betzios, N. Gaddam, and O. Papadoulaki, Black holes, quantum chaos, and the Riemann hypothesis, *SciPost Phys. Core* 4, 032 (2021).
- [45] T. Morita, Thermal Emission from Semiclassical Dynamical Systems, *Phys. Rev. Lett.* 122, 101603 (2019).
- [46] K. Takahashi and N. Saitô, Chaos and Husimi Distribution Function in Quantum Mechanics, *Phys. Rev. Lett.* 55, 645 (1985).
- [47] Shangyun Wang, Songbai Chen and Jiliang Jing, Effect of system energy on quantum signatures of chaos in the two-photon Dicke model, *Phys. Rev. E* 100, 022207 (2019).
- [48] S. Chaudhury, A. Smith, B. E. Anderson, S. Ghose and P. S. Jessen, Quantum signatures of chaos in a kicked top, *Nature (London)* 461, 768 (2009).
- [49] A. Piga, M. Lewenstein and J. Q. Quach, Quantum chaos and entanglement in ergodic and nonergodic systems, *Phys. Rev. E* 99, 032213 (2019).
- [50] V. Mourik et al, Exploring quantum chaos with a single nuclear spin, *Phys. Rev. E* 98, 042206 (2018).
- [51] K. Furuya, M. C. Nemes, and G. Q. Pellegrino, Quantum Dynamical Manifestation of Chaotic Behavior in the Process of Entanglement, *Phys. Rev. Lett.* 80, 5534(1998).
- [52] See Supplemental Material at <http://link.aps.org/supplemental/10.1103/PhysRevE.101.010202> for details.
- [53] A. I. Larkin and Yu. N. Ovchinnikov, *Zh. Eksp. Teor. Fiz.* 55, 2262 (1969) [*Sov. Phys. JETP* 28, 1200 (1969)].
- [54] J. Chávez-Carlos, Classical chaos in atom-field systems. *Phys. Rev. E* 94, 022209 (2016).